CHALMERS
UNIVERSITY OF TECHNOLOGY

Hole-mask lithography for fabricating bielement nanoplasmonic metasurfaces

Master's thesis in nanotechnology

Harald Ottedag

THESIS FOR THE DEGREE OF MASTER OF SCIENCE OF NANOTECHNOLOGY

Department of Physics
CHALMERS UNIVERSITY OF TECHNOLOGY
Gothenburg, Sweden 2018

Hole-mask lithography for fabricating bielement nanoplasmonic metasurfaces
Harald Ottedag
Göteborg 2018

Supervisor: Ferry Nugroho, Chemical Physics
Examiner: Christoph Langhammer, Chemical Physics

Department of Physics
Chalmers University of Technology
SE-41296 Göteborg
Telephone +46 (0)31 772 1000

Abstract

Hole-mask colloidal lithography (HCL) has been used extensively to fabricate arrays of nanostructures with uniform physicochemical traits, e.g. in size, shape and material, on a surface. A new way to create a metasurface with nanostructures with more than one physiochemical trait, for instance both gold and silver, each with different dimensions and/or aspect ratio, is suggested and tried. The possible applications of such a surface lies in the field of plasmonics for both fundamental and application aspects such as probing two different processes simultaneously, for instance temperature change and adsorption of molecules onto the surface. In this thesis the fabrications were unsuccessful in creating such a device, but significant progress was made in developing the method. Furthermore, characterisation of dual-size surfaces fabricated through HCL comprising silver discs was done. Specifically the relationship between mean center-to-center distance between nanoantennas, and plasmonic resonance wavelength was investigated.

Contents

1 Introduction

Alchemy, the precursor to modern chemistry, is the study of the transformation of mind, matter and soul.[1] The most well-known transformation is that of turning lead into gold; the turning of something base into something noble. This part of alchemy has survived modernisation and remains integral to chemistry; sand is turned into glass for touch screens, and rust made into contrast agents for magnetic resonant imaging.[2] It is at the heart of modern culture; the obligation to recycle and view waste as potential. Something as simple as stained glass in old churches holds both beauty and the possibility for deeper knowledge. Interspersed in the such glass are nanoparticles, and through their interaction with light the material exhibits different colours. In previous times it was known that fusing glass with gold makes it becomes red, with silver yellow and with nickel blue.[3] In reality the shape and size of the nanoparticles are also important factors, not only their element. Beneath the colours exists a foundation of lucrative science, a field of plasmonics and nanotechnology. With the right method it is possible to fabricate devices that detect changes in their immediate environment using the same acting forces as in stained glass. This type of device is known as a **nanoplasmonic surface**, of which the fabrication and characterisation are the topics of this thesis.

1.1 Project Aim

The Langhammer research group at Chalmers University of Technology has previously developed a hole-mask lithography method for fabricating differently shaped nanostructures comprising desired chemical species on a surface. In a single fabrication these nanostructures were of more or less identical shape and size. The method was further developed by creating nanostructures of two sizes by employing two sets of differently sized beads. The next step is to create a surface comprising nanostructures of more than one element, for instance both gold and silver. This is the goal of the project; to fabricate such a surface. The possible applications of such a surface lies in the field of plasmonics for both fundamental and application aspects. Probing two different processes, such as temperature change and adsorption of molecules onto the surface, simultaneously is a possibility. Furthermore, characterisation of monoelement surfaces with two disc sizes is done, specifically the relationship between mean center-to-center distance between nanoantennas, and plasmonic resonance wavelength is investigated.

1.2 Lithography

Key words:

- Top-down/bottom-up
- Hole-mask colloidal lithography

Lithography is used to fabricate nanoplasmonic surfaces and can be categorised as either top-down or bottom up. The former uses a mask to either create a pattern of its direct shadow, or the shadow's negative. Following is a simple **top-down** process:

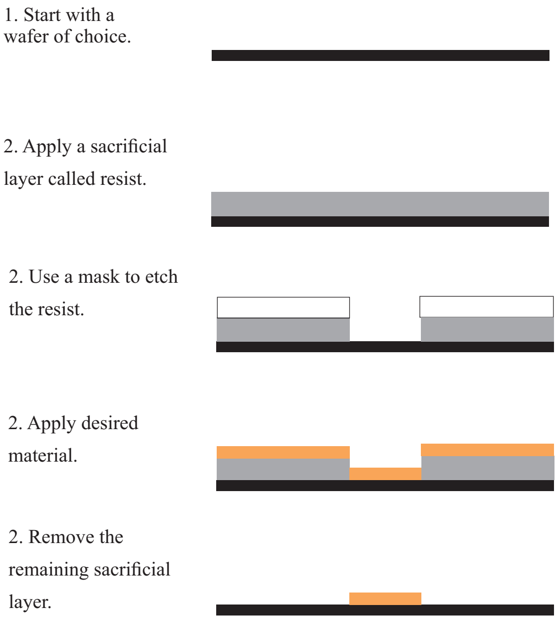

Figure 1: General top-down lithographic process.

This approach is most useful when an exact and known pattern such as a circuit or image is desired. Photolithography uses light to make the imprint of the mask. It is fast because the entire surface is exposed in one go as the entire surface is written simultaneously. This is why it is called parallel writing. In order to reduce the effect of light diffraction, which is the limiting factor for resolution, implementing lower wavelengths of light such as ultraviolet is common.[4] Using light is not the only way of performing parallel writing. Creating a stamp of a pattern and then imprinting it into a soft material is also possible. This is known as soft lithography. Because the method is cheap and the detail level of the pattern high, it is one of the most commonly used.[5]

Another way to perform lithography is to use a single focused point to draw a pattern by what is called sequential writing. Electron beam lithography is an example of this, where a single electron beam imprints a pattern directly into the resist, allowing a desired material to be deposited there. On one hand it achieves a higher resolution than photolithography because it is not limited by diffraction, but on the other hand it requires more time and is expensive. An outline of the lowest minimum feature size variants of the discussed lithographic methods is found in table 1.

Technique	Minimum feature size	Writing method	Area	Cost	Time
Extreme UV	<50 nm	Parallel	Large	High	Short
Electron Beam	1 nm	Sequential	Small	High	Long
Soft	10 nm	Parallel	Large	Low	Short

Table 1: Characteristics of some advanced lithographic techniques. Adapted from Colson et al.[6]

Bottom-up processes do not have pre-defined patterns, instead they let physical laws determine the mask's shape. Colloidal lithography is such a process, where a surface is covered by colloidal spheres that define the pattern through their electrostatic interactions. The pattern created by these spheres creates a deposition mask, as seen in figure 2. Employing different strategies, colloidal lithography can be used to fabricate a multitude of structures. For instance, by using two layers of spheres it is possible to create dots, as shown in figure 2.

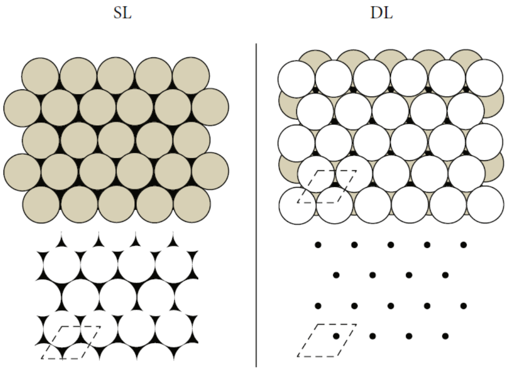

Figure 2: Bottom-up colloidal sphere mask and resulting pattern. SL: Single layer. DL: Double layer. Adapted from Colson et al.[6]

Any process that has a self-assembled mask is considered bottom-up, of which many are using colloidal particles. The bottom-up process of **hole-mask colloidal lithography**, developed by Fredrikson et al.,[7] is the method of choice for this project. In it a negatively charged surface exposed to a solution with polystyrene (PS) beads that electrostatically interact with the surface. Since the beads have the same charge they will repel one another and spread on the surface without significant agglomeration, creating a pattern with spacing following a normal distribution, seen in figure 7. To decrease the spacing, the concentration of PS in the applied solution can be adjusted. When the PS beads have been applied the surface is covered with a mask and the beads tape-stripped. The resulting hole-mask can be seen in figure 3. This makes for a powerful tool for manipulating plasmonic resonance by altering the size of the beads or changing their surface density by having a higher concentration solution. The underlying theory for this is covered in the following chapter on plasmonics.

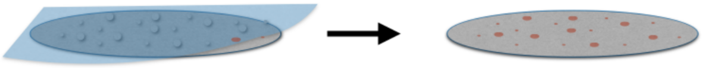

Figure 3: Hole-mask colloidal lithography where polystyrene spheres constitute a mask which is removed by tape-stripping. Taken from Developing a Nanoplasminic Ruler by O'Reilly.[8]

1.3 Fundamental plasmonics

Key words:

- Surface plasmon
- Local surface plasmonic resonance (LSPR)
- Plasmonic ruler

Conductive electrons in a material are not bound to local points. If excited by an external electric field, their coherent collective movements are called plasma oscillations. They are the coherent motions of negative electrons attracted to stationary positive lattice points. This results in oscillations with resonance frequencies that depend on the size of the system (number of lattice points) and the conductive electron density.[9] A plasmon is such a mode, a quasi-particle quantization of motion, energy and position expressed as the movement of a fluid.[10] Should the oscillations occur at an interface between a conductive material and a dielectric, they are called **surface plasmons**. The frequency of the oscillations is called plasma frequency ω_p. Following is the widely used Bohm-Gross model for the plasma frequency. It asserts that it is a combination of bulk electron movement ω_{cold} and thermal effects $\omega_{thermal}$ that can be interpreted as a second order correction term.[11]

$$\omega_p^2 = \omega_{cold} + \omega_{thermal} = N\frac{e^2}{m_e\epsilon_0} + k^2\frac{3K_bT}{m_e} \tag{1}$$

Here N is the number of electrons, e is elementary charge, m_e is electron mass, ϵ_0 is permittivity of vacuum, K_b is Boltzmann constant and k. If the electron bulk is viewed as a gas, an increase in temperature also increases the pressure, which can be understood as increasing the restorative force of the coupled motions. If the thermal term can be omitted, which is the case for the systems considered,[8] the model becomes:

$$\omega_p^2 = N\frac{e^2}{m_e\epsilon_0} \tag{2}$$

Should light shine on a plasmonic surface, a number of things can occur. The light could scatter, the material absorbing parts of the photon angular momentum and letting the them propagate in different directions. Or the material could absorb the photons, where their individual kinetic energies matches electron energy level differences. Should the photon energy and momentum match those of plasmons, plasmonic resonance would ensue.[12] When the oscillations caused by the light are contained in a structure and do not propagate, it is called **local surface plasmonic resonance** (LSPR).[13] It is dependent upon the materials present in the interface (plasmonic material and dielectric). As such, should one have a plasmonic material and be able to vary the dielectric, it is possible to control the plasmon resonance frequency, and hence which wavelengths of light are able to cause resonance. Thus the plasmonic surface can act as a detector where the input is the dielectric environment and the output is the resonance wavelength. Following is the relationship.

$$\omega_{LSPR} = \frac{\omega_p}{\sqrt{1 + 2\epsilon_{medium}}} \tag{3}$$

Here ϵ_{medium} is the dielectric constant of the surrounding medium.

2 Method

There are two distinct methods employed in this thesis. First is the development of a surface comprising two different nanoantennas types, comprised of two different metals and with different sizes. The discussion includes a complete overview of the method and details of which fabrication steps need improvement. Second is the fabrication of surfaces comprising silver nanodiscs of two different sizes.

2.1 Surface with antennas of two different metals and sizes

The fabrication scheme of this surface is shown in figure 4. It is an adaptation of the method described by O'Reilly.[8] The key steps that still need development for the method to work are 3 and 8: tape-stripping only large beads and the removal of the sacrificial layer without etching the plasmonic materials. To develop the surface it is therefore a matter of discovering a way to strip only one bead size, and finding a suitable etchant-sacrificial layer pair. Following the steps in figure 4, this was the attempted method for creating the surface.

1. Applying resist and PS beads on substrate.

Silicon substrates were cleaned with acetone, IPA and water for 3 min each with sonication and nitrogen-drying in-between each step. PMMA 950 A4 was spincoated onto the substrates at 2000 rpm for 1 min to ensure a flat and even surface roughly 275 nm thick. Baking for 5 min at 170 °C was then done. Oxygen reactive ion etching for 5 s was then performed to increase hydrophilicity in order for the subsequent step of depositing a polyelectrolyte polydiallyldimethylammonium (PDDA) monolayer to succeed. PDDA was added to the samples for 40 s and then washed for 20 s with water, and dried with nitrogen. Lastly the PS beads were pipetted onto the surface and left for 3 min after which the samples were rinsed for 20 s with water.

2. Evaporation of hole-mask

In order to add a thin hole-mask to the sample, a Lesker e-beam physical vapour deposition (eBPVD) was used. It applied a uniform film of chromium of desired thickness. The most common thickness was 15 nm, but this was also varied in one of the attempts to make the tape-stripping in the next step to work.

3. Tape-strip large beads

Tape was applied evenly onto the sample and the stripping performed with a smooth and even motion. The tape used for most experiments was SWT-10, but other brands were also tried including scotch and kapton. More details on tape-stripping are found in the results section.

4-8. *These steps were never reached since the tape-stripping removed both types of beads in all cases. Detail level is therefore lower.*

4. Etch away resist.

The PMMA resist is to be etched with oxygen plasma for 5 min in order to ensure that all of the exposed resist is removed.

5. Deposit first plasmonic material and sacrificial layer.

The plasmonic material for the large size discs and a sacrificial layer are to be deposited, in that order and by evaporator.

6. Tape-strip small beads.

Tape-stripping of smaller beads is to be done using the same technique and tape as step 3.

7. Deposit second plasmonic material.

Deposit the plasmonic material for the small size disc the same way as step 5.

8. Lift off resist and sacrificial layer

Lift off the resist using acetone, and sacrificial layer using a matching etchant.

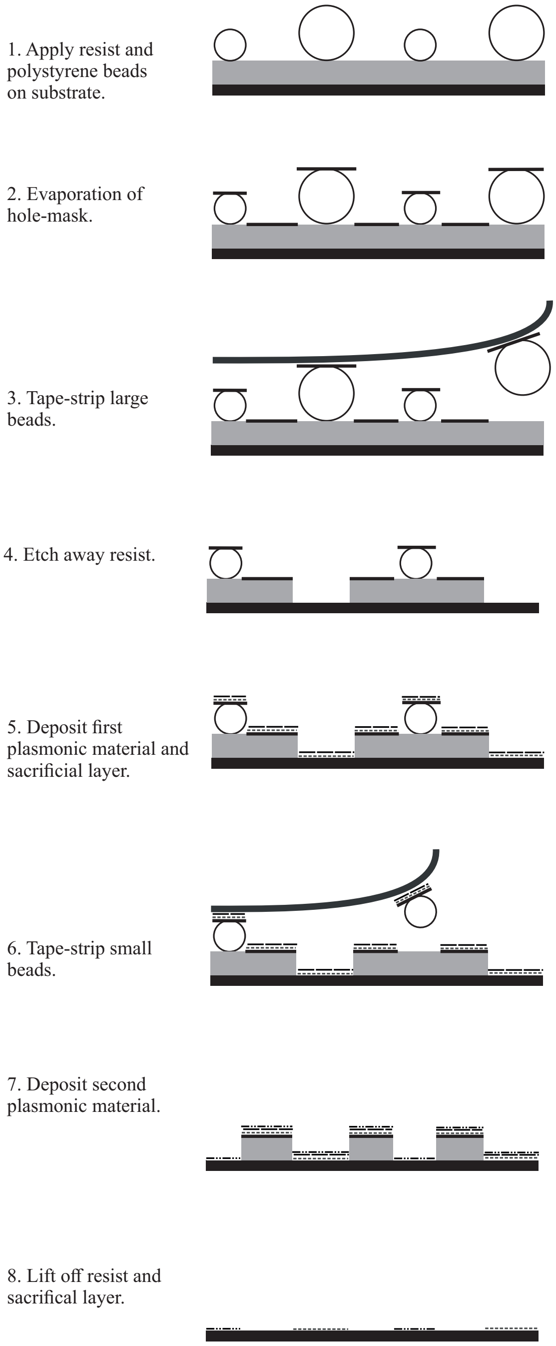

Figure 4: Fabrication schematic for generating a metasurface of plasmonic metal nanoparticles of up to two compositions.

2.2 Dual-size silver nanodisc surface

Fabrication of dual-size monoelement surfaces of silver discs follows the method described exactly in O'Reilly.[8] The method description accompanies the schematic shown in figure 5. The samples were made on both silicon and silica to be characterised by SEM and spectrophotometry, respectively.

1. Deposition of sacrificial resist layer and masking colloids.
Substrates were cleaned with acetone, IPA and water. PMMA 950 A4 was spun onto the to create a flat and even surface 275 nm thick. Baking for 5 min at 170 °C was then done. Reactive ion etching for 5 s was then performed. PDDA was added to the samples for 40 s and washed with deionised water. Lastly the PS beads were pipetted onto the surface and left for 3 min after which the samples were rinsed with deionised water.

2. Evaporation of hole-mask
A thin mask was evaporated onto the sample using Lesker e-beam physical vapour deposition (eBPVD). A uniform 15 nm film of chromium was applied.

3. Tape-strip all beads
Tape was applied evenly onto the sample and the stripping performed with a smooth and even motion. Stripping was done twice to ensure that all beads were removed. The tape used was SWT-10.

4. Oxygen plasma etch.
The PMMA resist is to be etched with oxygen plasma for 5 min in order to ensure that all of the exposed resist is removed.

5. Materials evaporation (silver).
20 nm of silver was evaporated into the etched holes using eBPVD.

6. Lift-off in acetone.

Remaining mask and PMMA were removed by lift-off with acetone.

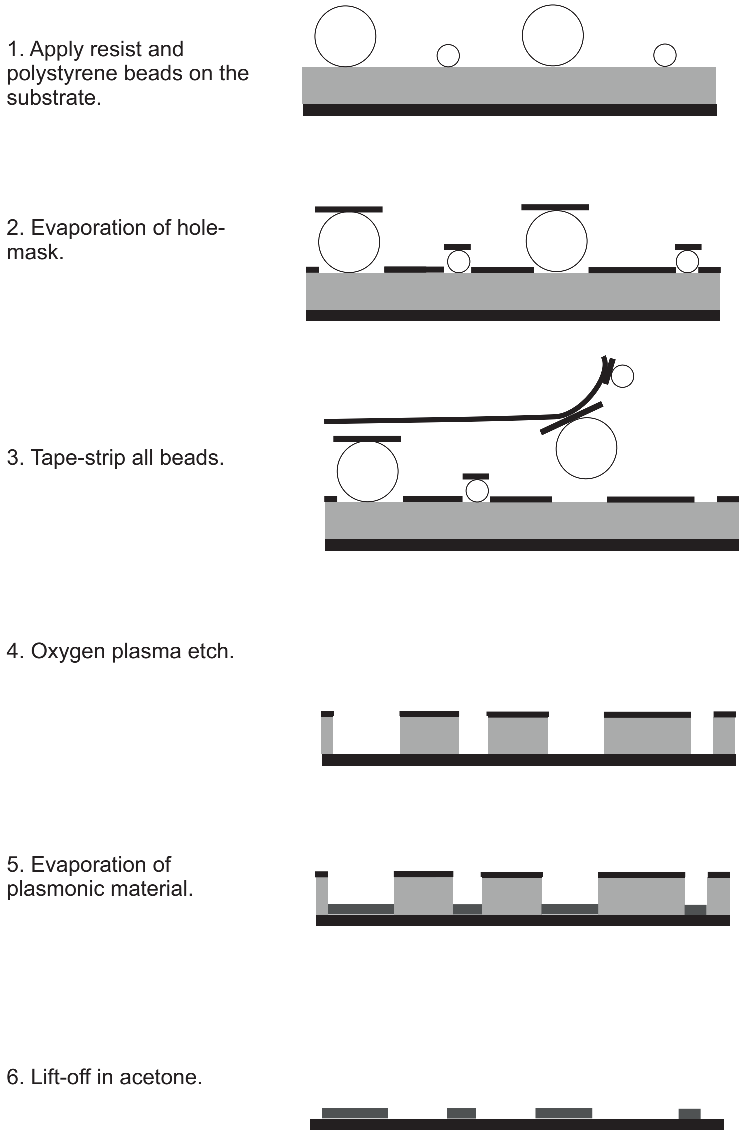

Figure 5: Hole-mask colloidal lithography method for generating monoelement metal nanoparticles of two sizes. The material deposited was silver. The resulting surface was silver discs of one size.

3 Characterisation

3.1 Scanning electron microscopy

Scanning electron microscopy (SEM) is used to characterise composition and topography of a solid sample by shining an electron beam at it. It can confirm the success of a fabrication by showing the spread of the nanodiscs. Unwanted agglomeration, the result of poor PS solution quality, is easily identified as clusters. SEM operates by translating electron beam interactions with the sample into an image where shade indicates composition and topography. Topographical information is mainly given by secondary electrons (SE) that are remitted back from the sample.[14] and the angle of emission for SE can be high so the position of the sample relative to the detector important. The topography of a pollen sample can be seen in figure 6a where height is shown by the shading. For composition, a brighter shade is a direct result of more electrons being detected. This is mainly from electrons that scatter to a detector behind the sample. For this reason they are called backscatter electrons and are the main source for compositional information.[14] Compositional information is then translated into contrast. Gold, for instance, is bright and carbon is dark, as seen in figure 6b.[15]

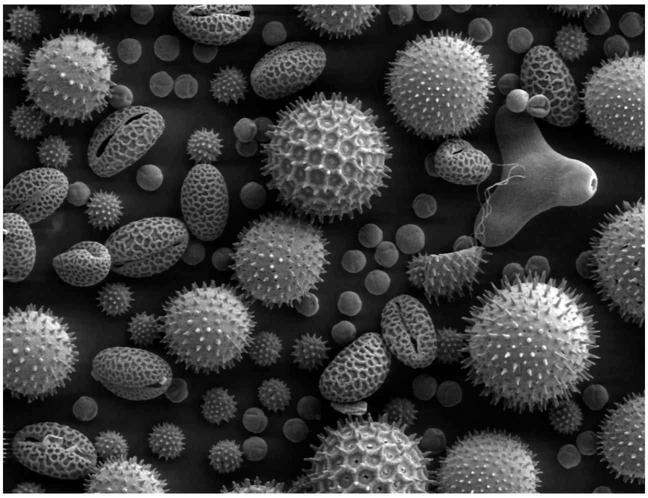

(a)

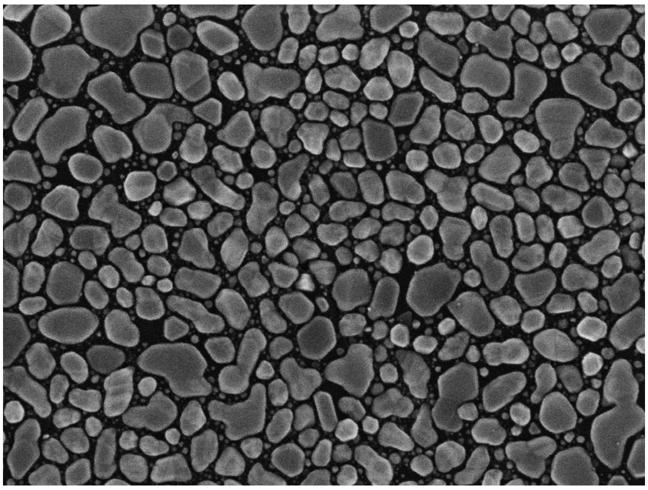

(b)

Figure 6: SEM images of pollen (a) and gold flakes on carbon (b) to illustrate that SEM shows height and distinguishes between composition by intensity of brightness and contrast. Images are from Wikimedia Commons.

In this project SEM has two main roles: to confirm the success of a fabrication, and to measure the mean centre-to-centre distance d_{mean}. For the latter only mean distance between same-size beads is considered, that is between small and big beads separately. In order to calculate d_{mean} image processing has to be performed. ImageJ is used for this and an example of the process can be seen in figure 8. The image is made binary, isolating the beads to allow distances between points to be measured. It from the resulting images that the minimum centroid distances d_{min} for each particle can be found. Unsurprisingly, d_{min} roughly follows a normal distribution, as can be seen in figure 7. Each distribution reflects one SEM-image of a bead concentration set, and it is the mean value of each distribution that is sought. The definition of d_{mean} is:

$$d_{mean} = \frac{1}{n} \sum_{n} d_n \tag{4}$$

where n is the total number of particles and d_n is $d_m in$ for each particle. Plotted against the plasmonic wavelength at resonance λ_p, it is used to characterise the surfaces. In order to have a sufficiently big sample size two images per concentration set are used. The sample size then amounts to over 3000 for small-to-small distances and over 800 for big-to-big.

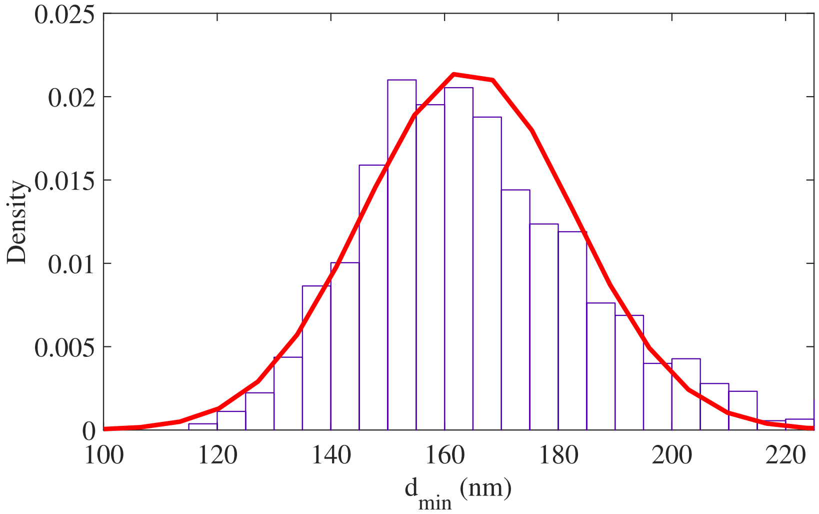

Figure 7: Estimate of the probability distribution of d_{min}. The normal distribution parameters are $\mu = 164.2.4$ nm, $\sigma = 18.5$ nm.

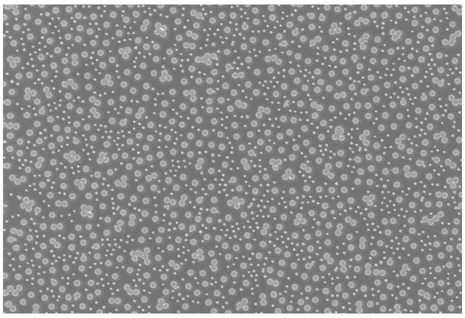

(a) Before image processing.

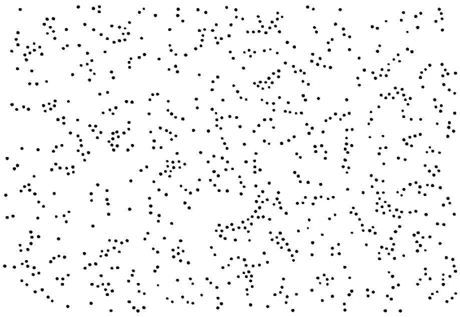

(b) Only $d = 80$ nm discs.

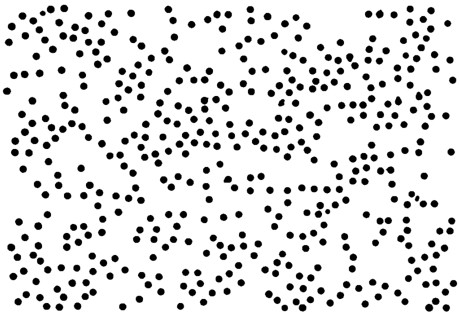

(c) Only $d = 200$ nm discs.

Figure 8: The process of making SEM images binary to allow for determination of d_{min}. The original SEM image is shown in (a). (b) and (c) show the resulting binary images with only d=80nm and d=200nm discs, respectively.

3.2 Spectrophotometry

In spectrophotometry light is sent through a sample and the difference in wavelength composition between input and output light is analysed.[16] Plasmon-photon interactions occur at certain energies corresponding plasmonic resonance, explained in section 1.3. These energies, expressed as wavelengths, are called plasmonic resonance wavelengths λ_p and can be identified as peaks in an extinction spectrum.[17] With two different sizes, each size corresponds to one peak, as illustrated in figure 9. Note that the figure shows the extinction $1-T$, where T is the portion of light that travels through the sample unhindered. By using absorption spectroscopy to record changes in λ_p when bead solution concentrations are varied it could be possible to see a relationship between d_{mean} and λ_p.

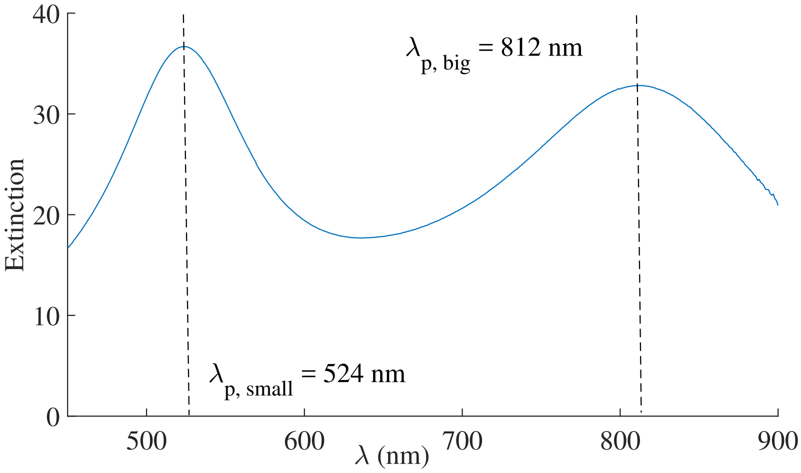

Figure 9: Example of the transmission spectrum of dual-size silver nanodisc surface. This surface was made with bead concentrations $C(small) = 0.0125$ w% and $C(big) = 0.15$ w%. LSPR peaks with wavelengths λ_p for big beads of d=200 nm size and small beads of d=80 nm are indicated by dotted lines.

4 Results

4.1 Creating a bielement surface

There were two main challenges in creating the bielement surface: To make the tape-stripping only remove large beads during the first strip, and having a selection of etchants for the sacrificial layer that does not etch away the plasmonic materials. Unfortunately first challenge was not overcome and as such the method development did reach the second challenge. However, many different attempts at successful tape-stripping of only the large beads were made. Each of the following subchapters details a different avenue of approach, with sample parameters found in the beginning and SEM images of the tape-stripping results.

4.1.1 Changing bead solution concentrations

Sample	C(big) w%	C(small) w%	Size(big) nm	Size(small) nm	Tape	Cr mask (nm)
1	0.1	0.01	200	80	SWT-10	15
2	0.1	0.015	200	80	SWT-10	15
3	0.1	0.02	200	80	SWT-10	15
4	0.125	0.01	200	80	SWT-10	15
5	0.125	0.015	200	80	SWT-10	15
6	0.125	0.02	200	80	SWT-10	15
7	0.15	0.01	200	80	SWT-10	15
8	0.15	0.015	200	80	SWT-10	15
9	0.15	0.02	200	80	SWT-10	15
10	0.2	0.2	200	80	SWT-10	15
11	0.3	0.01	200	80	SWT-10	15
12	0.35	0.01	200	80	SWT-10	15

Table 2: surface fabrication parameters.

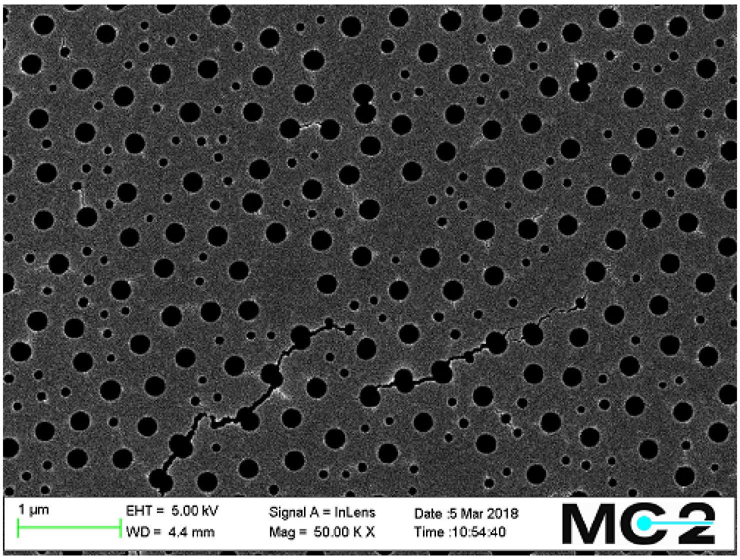

Figure 10: SEM image of sample 11 from table 2 showing tape-stripping of all beads.

The first attempt was to vary the concentrations of the PS bead solutions. It was reasoned that with a sufficiently high surface density of large beads, the tape would be prevented from reaching the small beads. However, even the highest concentration differences proved unsuccessful. Perhaps electrostatic attraction between bead and tape made direct contact unnecessary; or the tape was not rigid enough and therefore managed to reach in-between the large beads. If the tape were only slightly soft, increasing the bead size difference would compensate for it sinking in-between the beads. This was the next approach, to increase the big bead size.

4.1.2 Maximizing bead size difference

Sample	C(big) w%	C(small) w%	Size(big) nm	Size(small) nm	Tape	Cr mask (nm)
1	0.15	0.01	230	80	SWT-10	15
2	0.15	0.01	250	80	SWT-10	15
3	0.15	0.01	300	80	SWT-10	15

Table 3: surface fabrication parameters.

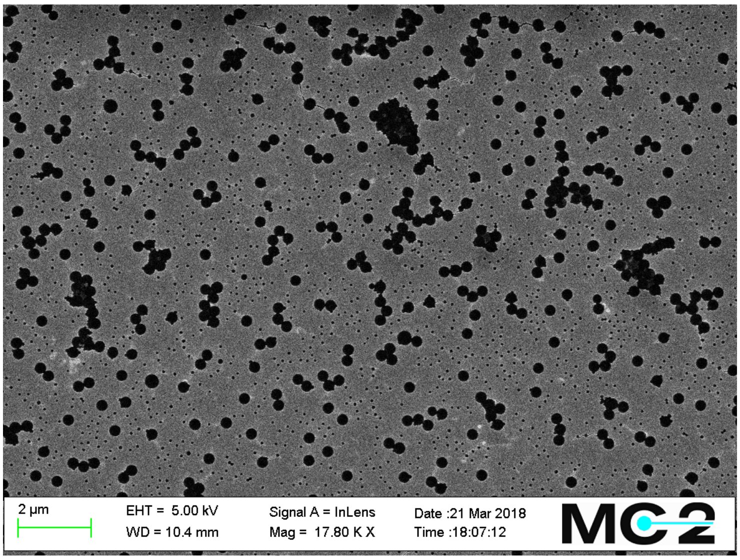

Figure 11: SEM image of sample 3 from table 3 showing tape-stripping of all beads.

The second approach was to increase the bead size difference. The small bead diameter was held at 80 nm and the large bead diameters varied. It was thought that the tape would not be able to reach far enough in-between the large beads to touch the small beads provided that the big bead diameter was sufficiently large. However, all beads were stripped regardless of size. Again maybe electrostatic attraction between bead and tape forced the beads onto the tape, or the tape was actually a softer surface than envisioned. If the tape was soft, perhaps the act of pushing down onto the tape forced it in-between the large beads. Therefore the next area of investigation was the tape-stripping technique.

4.1.3 Tape-stripping technique

Sample	C(big) w%	C(small) w%	Size(big) nm	Size(small) nm	Tape	Cr mask (nm)
1	0.15	0.01	230	80	SWT-10	15

Table 4: surface fabrication parameters.

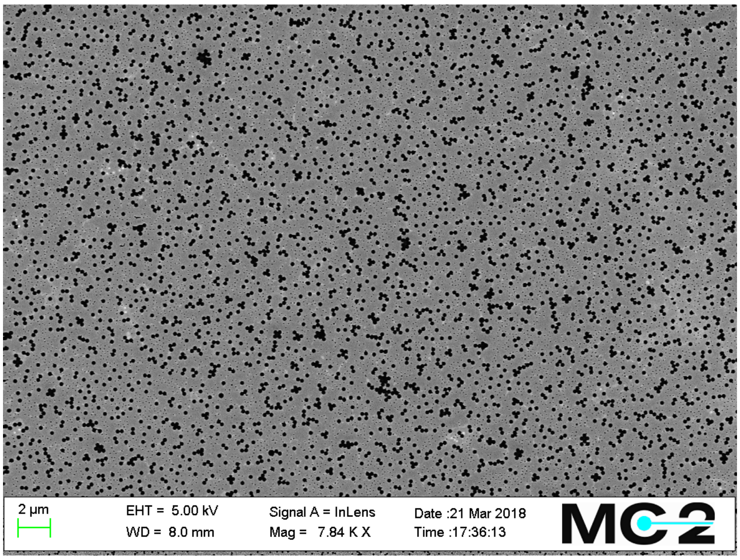

Figure 12: SEM image of sample 1 from table 4 displaying tape-stripping of all beads.

The third investigated strategy was to change the tape-stripping technique. The previously used technique was to apply the tape and push down on it gently with a finger. Perhaps the act of pushing down on the tape actually pressed it in-between the larger beads and onto the small ones, thus forcing contact with all beads. Therefore a technique where the tape was applied without any pressure, i.e. just letting it fall onto the surface, was tried. Unfortunately this did not work either and once again the stripping did not discriminate between bead sizes. At this stage the most rational conclusion was that the beads were attracted electrostatically to the tape. The next approach was therefore to test tapes with different electrostatic properties.

4.1.4 Different tape

Sample	C(big) w%	C(small) w%	Size(big) nm	Size(small) nm	Tape	Cr mask (nm)
1	0.15	0.01	230	80	Cloth, glass	15
2	0.15	0.01	230	80	Kapton	15
3	0.15	0.01	230	80	Scotch magic	15
4	0.15	0.01	230	80	Scotch vinyl	15
5	0.15	0.01	230	80	WBT-EF030	15

Table 5: surface fabrication parameters.

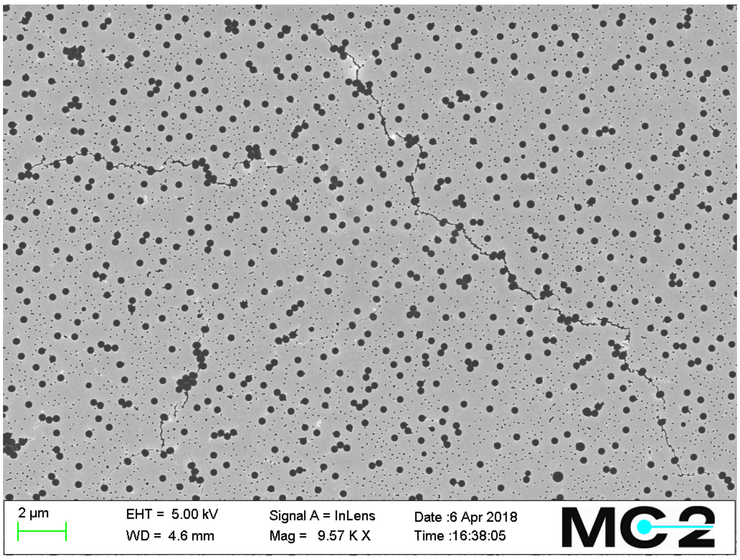

Figure 13: SEM image of sample 3 from table 5 displaying tape-stripping of all beads.

The fourth try was to use different tapes. It was thought that the tape electroscatically attracted the small beads, and as such a change of tape could allow for a lower attraction level. An array of different tapes was assembled and the aforementioned softer tape-stripping technique was also tried. Unfortunately all tapes stripped indiscriminately of bead size and technique. It could be the case that the only way of preventing the tape from pulling the smaller beads was to hold them firmly to the surface. It was with this line of reasoning that the next avenue of approach became increasing the thickness of the chromium mask.

4.1.5 Chromium mask thickness

Sample	C(big) w%	C(small) w%	Size(big) nm	Size(small) nm	Tape	Cr mask (nm)
1	0.15	0.01	200	80	SWT-10	30
2	0.15	0.01	200	80	SWT-10	40
3	0.15	0.01	200	80	SWT-10	50
4	0.15	0.01	200	80	SWT-10	60
5	0.15	0.01	200	80	SWT-10	62
6	0.15	0.01	200	80	SWT-10	64
7	0.15	0.01	200	80	SWT-10	66
8	0.15	0.01	200	80	SWT-10	68
9	0.15	0.01	200	80	SWT-10	70
10	0.15	0.01	200	80	SWT-10	80

Table 6: surface fabrication parameters.

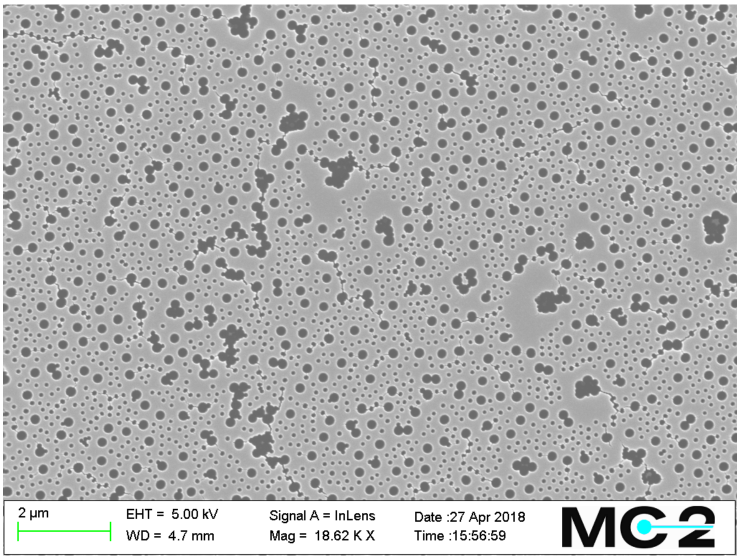

(a) 40 nm Cr

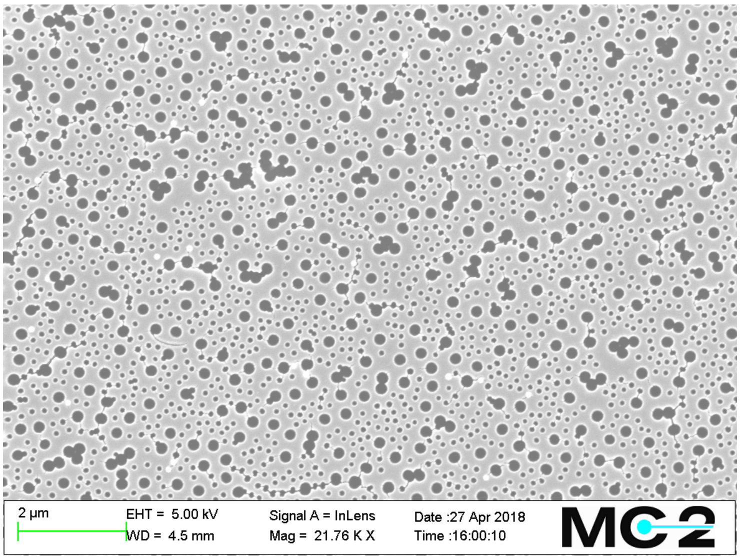

(b) 50 nm Cr

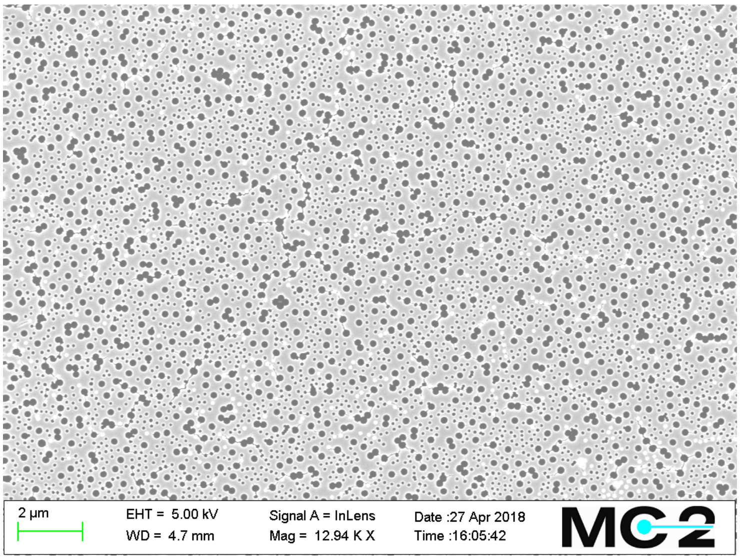

(c) 60 nm Cr

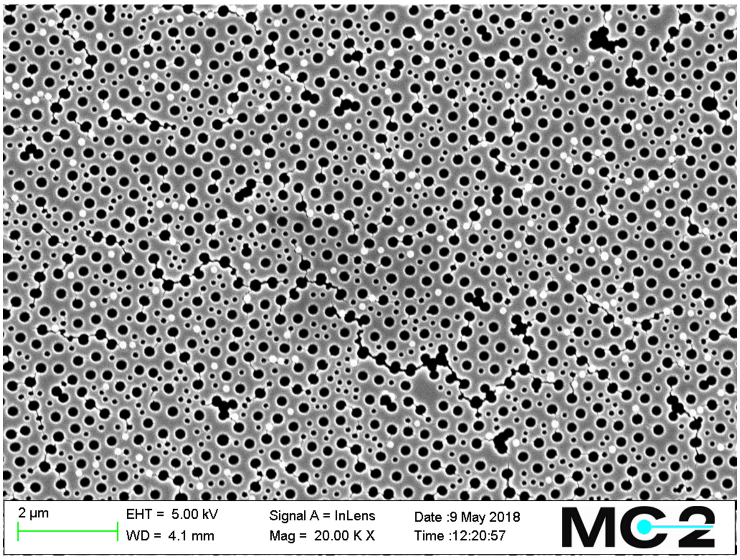

(d) 70 nm Cr

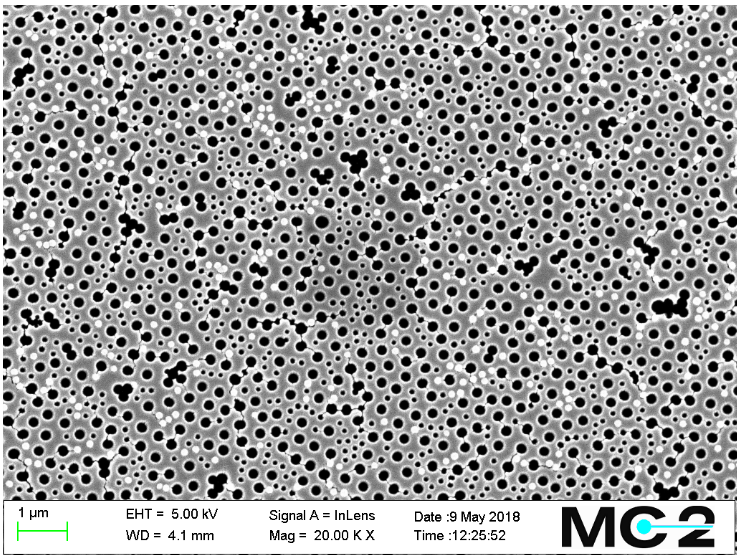

(e) 80 nm Cr

Figure 14: SEM images of samples from table 5 of increasing chromium mask thickness. Black circles are stripped beads, white circles are unstripped.

For the final attempt the chromium mask's thickness was increased. It was reasoned that to block the small beads from being stripped, the small beads could be covered partially or completely by the chromium mask. For the lower mask thicknesses all beads were still stripped, but for thicknesses above 50 nm there were unstripped beads. By inspection it could also be seen that with increased mask thickness there were fewer stripped small beads. At 80 nm thickness, the diameter of the small beads, a great amount of beads were unstripped . It could be that because of the statistical size distribution of the bead solutions, those that are below $d = 80$ nm were not stripped since they were completely covered by the mask. The remaining beads were larger and thus not covered by the mask. The natural continuation is to increase the mask thickness until all small beads resist the tape-stripping. From this point it is a matter of being able to strip a second time, which is explored in the discussion section.

4.2 Characterising the dual-size surface

In order to characterise the dual-size surfaces, three series of PS bead concentrations with constant big bead concentrations and increasing small bead concentrations were made, details of which are found in table 7. They were then scanned with SEM and spectrophotometry in order to find the effects of increasing surface density of large and small beads on the plasmonic peak. This was done to investigate plasmonic coupling between the nanoparticles. The extinction spectra are found in figure 15 and λ_p of all samples are plotted against the mean d_{mean} in figure 16. The extinction measurements showed no apparent trends. When looking at figure 15c and the position of the higher wavelength plasmonic peak $\lambda_{p,big}$, going from C(80)=0.005 w% to 0.01 w% shows a shift to the right and a lowering of the peak. However when the small bead concentration increases further the trend breaks. Similar lack of trends can be found throughout the extinction spectra. Another example is the $\lambda_{p,small}$ in figure 15b that follows no trend at all. What can be said from the spectra is that the extinction at most depends on the bead concentrations in a very complex way, or not at all.

What the bead concentrations have a direct relationship to, however, is the d_{mean}, the mean center-to-center distance. Since the bead concentrations have no apparent relationship to the extinction spectra, so neither does d_{mean}. This can be seen from figure 16 which shows no identifiable trends. Antosiewicz et al.[18] investigated the extinction in relation to center-to-center distance in similar devices but with only one antenna size and found an oscillatory pattern. However from the experimental results of this thesis it is clear that the dual-size surface is much more complex.

There are a number of things that can be said about the extinction spectra. With increased small bead concentration the extinction increases, as can be seen by inspecting the left peak in figure 15b. This is reasonable since with a higher amount of nanoparticles, they are more likely to interact with the light. The same can be said about when the big bead concentration increases. The sharpness of the peaks also increases with concentration. This suggests that the coupled plasmonic motions more easily approached resonance frequency when the surface density of nanoparticles was higher.

Sample	C(big) w%	C(small) w%	Size(big) nm	Size(small) nm	Silver discs (nm)	Cr mask (nm)
1	0.05	0.005	200	80	20	15
2	0.05	0.01	200	80	20	15
3	0.05	0.0125	200	80	20	15
4	0.1	0.005	200	80	20	15
5	0.1	0.01	200	80	20	15
6	0.1	0.0125	200	80	20	15
7	0.1	0.015	200	80	20	15
8	0.15	0.005	200	80	20	15
9	0.15	0.01	200	80	20	15
10	0.15	0.0125	200	80	20	15
11	0.15	0.015	200	80	20	15

Table 7: surface fabrication parameters for dual-size silver nanodisc surfaces.

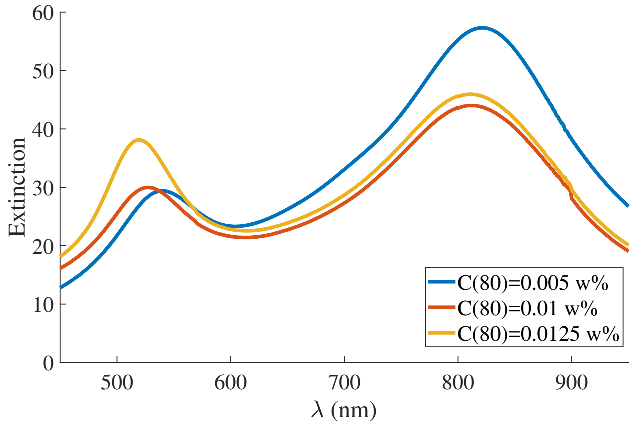

(a) C(200)=0.05 w%

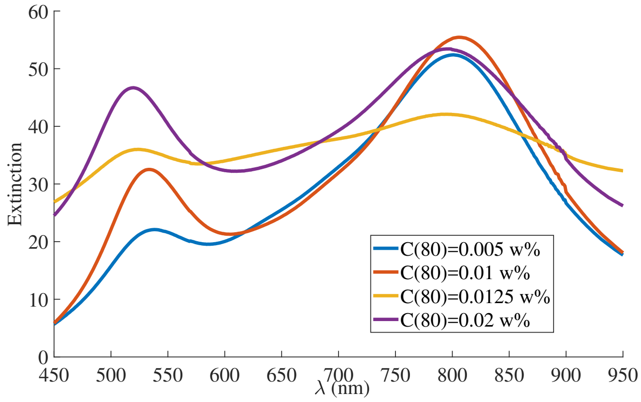

(b) C(200)=0.1 w%

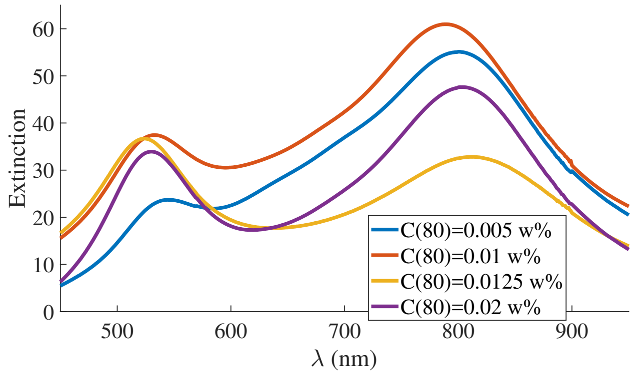

(c) C(200)=0.15 w%

Figure 15: Experimental results for extinction for dual-size silver surfaces. Concentrations C(80) and C(200) indicate PS bead solution concentrations of sizes 80 nm and 200 nm.

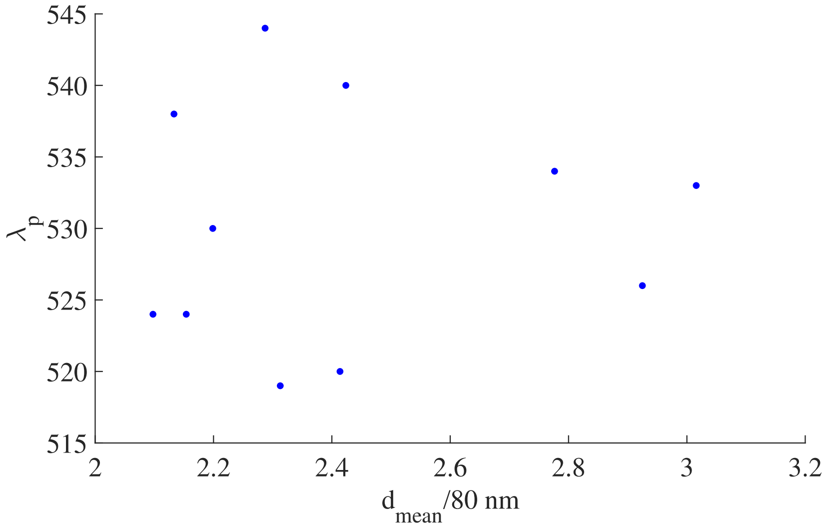

(a) Small particles.

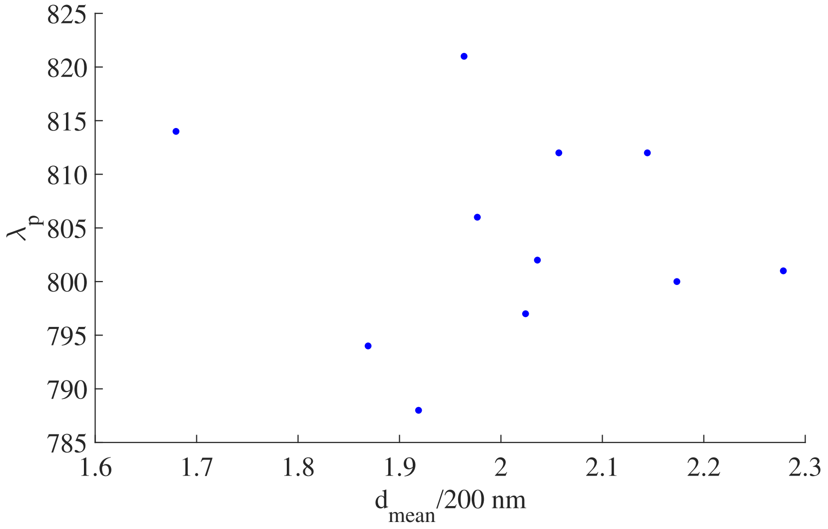

(b) Big particles.

Figure 16: Experimental results of plasmonic resonance wavelength λ_p as against mean center-to-center distance d_{mean}, in units of respective particle diameter. Distances between small particles (a) of d=80 nm and between big particles (b) of d=200 nm

5 Discussion

The attempts at creating a plasmonic surface with nanoparticles with two different metals and sizes indicate a number of things. Firstly that the tape stripping does not seem to need direct contact with the beads in order for them to adhere to it. This was seen in the second attempt where the size difference between the beads was increased and the concentrations kept high, but also in the first attempt where the concentration difference was maximized. There are two main options as to why the tape did not discriminate between sizes. Either the tape was soft enough for it to slip in-between the large beads to touch the small ones, or it strips mainly by electrostatic attraction. In either case the electrostatic attraction would have to be of a relatively great magnitude since in the final attempt, where the chromium mask thickness was increased, the small beads were stripped even when the mask was as thick as their radii. Pulling the beads out of the chromium must have required significant force. It is especially because of this last observation that it is more likely that the tape strips by electrostatically pulling the beads.

The second significant discovery in the fabrication of bielement surface is that with a sufficiently thick mask some beads were not stripped. It is therefore the natural next step to further increase the mask to the point where no small beads are stripped. Care has to be taken that the mask size does not prevent the large beads from being stripped. By looking at when the small beads stopped being stripped, which occurs in the vicinity of reaching 2/3 of the diameter, the mask thickness should not exceed 130 nm for the 80/200 nm bead size pair. Increasing the mask thickness from 80 nm to 120 nm in increments of 10 nm would therefore be advisable. This will completely cover a majority of small beads with chromium, but presenting the problem of stripping away embedded beads. This can be solved by using a chromium etch, which in turn risks dissolving the PMMA underneath the chromium layer. To address this, a protective layer matching the selectivity of the chromium etchant could be deposited, as illustrated in figure 17. Chromium etchants do not etch gold and silver, so they are possible candidates for the protective layer.[19] However, since the chromium etch will be used after the large beads have been removed, the PMMA underneath them is exposed to the etchant. If the chromium etchant removes PMMA at a high rate, then this risks removing the PMMA and exposing the substrate. The etchant would not only etch downwards, but also to the sides underneath the deposited layers, which could ruin the surface. A possible solution to this, provided the chromium etch speed for PMMA is slow, having a sufficiently thick PMMA layer would perhaps allow the chromium to be etched before too much damage is done. Alternatively, a resist more resistant to the chromium etch could be used in which case a protective layer is unnecessary.

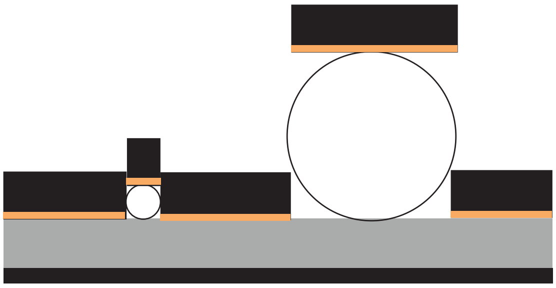

Figure 17: Suggested improvement of mask coverage step of having an protective layer to prevent chromium etch from reaching PMMA in the case where a thick mask is used. Layers are in order of top to bottom: Chromium, protective layer, PMMA, substrate.

Using this method of enabling tape-stripping by using a thick mask presents some limitations to the size difference of the beads. If it is too small, then both bead sizes would remain unstripped when the mask is applied. Finding the minimum allowed size difference will therefore be important since it will be the limiting factor in determining what possible nanoparticle size pairs can be created.

An alternative to completely cover the small beads in a mask is to strengthen the attraction between the PS beads and the surface. In the current schematic the PS beads rest on a polyelectrolyte monolayer of PDDA. If a stronger polyelectrolyte were used, then perhaps only partially covering the small PS beads with a mask would be enough to hold them in place. However, too strong a polyelectrolyte could prevent tape stripping altogether, which is undesirable.

Provided the tape-stripping of one bead size at a time works, it should only a matter of finding a suitable wet etchant and sacrificial layer pair (applied in step 5 in figure 4). Since the plasmonic materials will be exposed to the etchant, it is important that the etchant has the appropriate selectivity. If sufficiently noble metals such as gold and platinum used for plasmonic materials, then chromium is a viable sacrificial layer since some chromium etchants do not etch them. If a surface with three different nanoantennas is to be created then two sacrificial layers would have to be used, and as such two sufficiently selective etchants. This would severely limit the possible plasmonic materials that could be used. It should be possible to create such a device, but the fabrication method could then lack flexibility in the choice of plasmonic materials.

As for the characterisation of the dual-size silver nanoparticle surface, it could be the case that the fabrication method has a large range of outcomes for the devices it creates, meaning that if the exact same fabrication parameters are used, devices with very different characteristics are generated. If this is the case, the lack of trends would be an indication of that the measurements are done at a higher accuracy than allowed by the fabrication method. This point is strengthened by Antosiewicz et al.[18] where similar surfaces with only one size and one metal were made with e-beam lithography, which has great control over the placement of the particles. The method places particles based on a pre-defined radial distribution function which determines surface density and minimum center-to-center distance. Their results showed a sinusoidal relationship between minimum center-to-center distance and λ_p. The main difference between their devices and the ones created in this thesis by hole-mask colloidal lithography is that their method produces very similar devices each fabrication, whereas hole-mask lithography does not to the same degree. In order to pursue this avenue of investigation it would probably be best to first test how much the extinction spectrum varies with the same fabrication parameters. If the spectrum variations are sufficiently low then trying to correlate d_{mean} to λ_p is viable.

References

[1] Carl Gustav Jung. *Psychology and alchemy*, volume 12. Routledge, 2014.

[2] Ludovico Cademartiri and Geoffrey A Ozin. *Concepts of nanochemistry.* John Wiley & Sons, 2009.

[3] BG Brunetti, L Cartechini, C Miliani, and A Sgamellotti. Metal nanoparticles in glass: lustre. *Modern Methods for Analysing Archaeological and Historical Glass, Volume I*, pages 583–608, 2013.

[4] Shaoli Zhu, Yongqi Fu, and Junzhan Hou. Lithography: Principles, processes and materials. 2011.

[5] John A Rogers and Ralph G Nuzzo. Recent progress in soft lithography. *Materials today*, 8(2):50–56, 2005.

[6] Pierre Colson, Catherine Henrist, and Rudi Cloots. Nanosphere lithography: a powerful method for the controlled manufacturing of nanomaterials. *Journal of Nanomaterials*, 2013:21, 2013.

[7] Hans Fredriksson, Yury Alaverdyan, Alexandre Dmitriev, Christoph Langhammer, Duncan S Sutherland, Michael Zäch, and Bengt Kasemo. Hole–mask colloidal lithography. *Advanced Materials*, 19(23):4297–4302, 2007.

[8] Padraic O'Reilly. Development of a nanoplasmonic ruler. 2017.

[9] M Mitome, Y Yamazaki, H Takagi, and T Nakagiri. Size dependence of plasmon energy in si clusters. *Journal of applied physics*, 72(2):812–814, 1992.

[10] DB Mast, AJ Dahm, and AL Fetter. Observation of bulk and edge magnetoplasmons in a two-dimensional electron fluid. *Physical review letters*, 54(15):1706, 1985.

[11] David Bohm and Eugene P Gross. Theory of plasma oscillations. a. origin of medium-like behavior. *Physical Review*, 75(12):1851, 1949.

[12] Naomi J Halas and Thomas R Huser. Plasmonics: Metallic nanostructures and their optical properties ii. In *Plasmonics: Metallic Nanostructures and Their Optical Properties II*, volume 5512, 2004.

[13] Victor Anthony Garcia Rivera, OB Silva, Yannick Ledemi, Younés Messaddeq, and E Marega Jr. *Collective Plasmon-Modes in Gain Media: Quantum Emitters and Plasmonic Nanostructures.* Springer, 2014.

[14] Joseph I Goldstein, Dale E Newbury, Joseph R Michael, Nicholas WM Ritchie, John Henry J Scott, and David C Joy. *Scanning electron microscopy and X-ray microanalysis.* Springer, 2017.

[15] Ray F Egerton. *Electron energy-loss spectroscopy in the electron microscope.* Springer Science & Business Media, 2011.

[16] Donald L Pavia, Gary M Lampman, George S Kriz, and James A Vyvyan. *Introduction to spectroscopy.* Cengage Learning, 2008.

[17] Jonathan A Scholl, Ai Leen Koh, and Jennifer A Dionne. Quantum plasmon resonances of individual metallic nanoparticles. *Nature*, 483(7390):421, 2012.

[18] Tomasz J Antosiewicz, S Peter Apell, Michael Zäch, Igor Zorić, and Christoph Langhammer. Oscillatory optical response of an amorphous two-dimensional array of gold nanoparticles. *Physical review letters*, 109(24):247401, 2012.

[19] Perrin Walker and William H Tarn. *CRC handbook of metal etchants.* CRC press, 1990.